Investigation of mechanical and microstructural properties of pure copper processed by combined extrusion-equal channel angular pressing (C-Ex-ECAP)

Behzad Akbarzadeh[1] · Hamid Gorji[1] · Mohammad Bakhshi-Jooybari[1] · Roohollah Jamaati[2] · Mohammad Javad Mirnia[1]

Abstract

Severe plastic deformation processes (SPDs) have been developed over the past decades to produce bulky parts with proper mechanical and microstructural properties. Equal-channel angular pressing (ECAP) is a method in which a metal is subjected to severe plastic straining through simple shear. The combined extrusion-equal channel angular pressing (C-Ex-ECAP) is proposed in this paper as a new method of SPD. This process is a combination of extrusion and ECAP processes. The new process contains two shear zones which can lead to UFG structure in fewer passes compared with ECAP. In the proposed method, there is the capability of fabricating longer specimens because of the presence of the extrusion process. This investigation has been performed up to six passes, and the microstructural, mechanical, and electrical properties have been studied in the deformed workpieces. The samples produced in six passes of this process showed a 480% increase in yield strength compared to the annealed sample, and a decrease in grain size from 18 μm to 820 nm, as well as an increase in hardness from 41.8 to 125 HV. The electrical conductivity study also showed that the six-pass specimens had a 5% reduction in electrical conductivity compared to the annealed specimens.

Keywords Severe plastic deformation · Equal channel angular pressing · Mechanical properties · Microstructure · Electrical conductivity

1 Introduction

Due to the increasing progress in the electronics industry and the increase in the efficiency of electrical equipment, the need to improve the properties of conductive metals, such as achieving high strength while maintaining electrical conductivity, has been taken into consideration. Many researches have been performed to obtain high-strength conductive metals through alloying. This technique has a major limitation of the considerable reduction in electrical conductivity [1]. Therefore, it is necessary to present a method that, while maintaining the electrical conductivity, can increase the mechanical properties of copper as an important conductive metal. The generation and distribution of the density of dislocations at ambient temperature can simultaneously enhance the mechanical and electrical properties of materials [2].

Severe plastic deformation (SPD) is one of the methods in increasing the strength of metals without losing the electrical properties. Equal channel angular extrusion (ECAE) was introduced as an SPD technique in the 1995 [3] and later other methods have been developed, such as cycle extrusion compression (CEC), high-pressure torsion (HPT), torsion extrusion (TE), multi-directional forging (MDF), and incremental high-pressure torsion (IHPT). Although the electrical conductivity of pure copper is reduced because of the accumulation of lattice defects during the SPD, its strength is increased to the range of strength in the alloyed copper [1].

✉ Hamid Gorji
  hamidgorji@nit.ac.ir

1 Department of Mechanical Engineering, Babol Noshirvani University of Technology, Babol, Iran

2 Department of Materials Engineering, Babol Noshirvani University of Technology, Babol, Iran

Fig. 1 Schematic of half the C-Ex-ECAP process
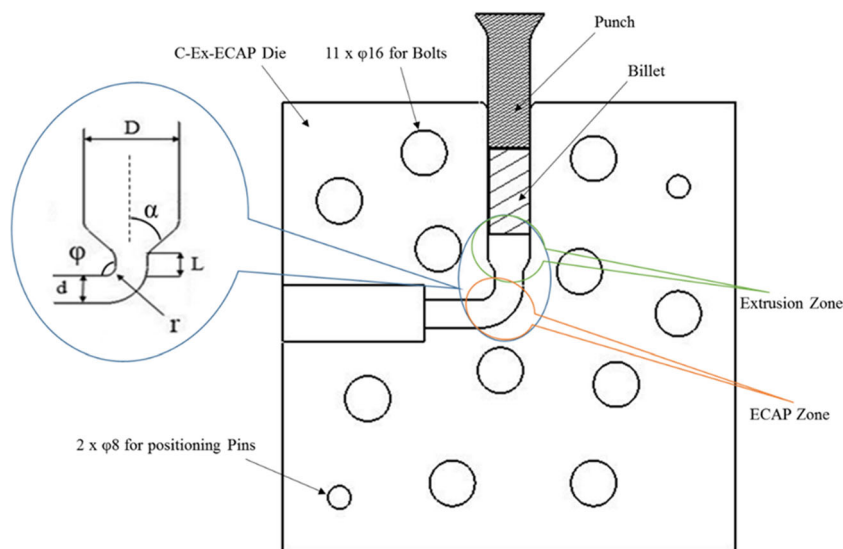
Wang et al. [4] proposed the elliptical cross-section spiral equal-channel extrusion (ECSEE) process as a novel SPD for fabricating nanostructure copper alloy. In this technique, the accumulated shear stress is applied to the workpiece without changing its cross-section. It was illustrated that after the first pass, the hardness of the specimen was significantly increased compared to the annealed state. In addition, significant grain refinement was observed. The equal channel forward extrusion (ECFE) process was presented by Ebrahimi and Djavanroodi [5]. They showed that after four passes on commercial pure copper in the annealed condition, yield strength (YS), ultimate tensile strength (UTS), and hardness of the sample were increased from 114 MPa, 204 MPa, and 68 HV to 269 MPa, 285 MPa, and 126 HV, respectively. Hohenwarter [6] proposed incremental high-pressure torsion

(IHPT) as a novel SPD method for fabricating UFG copper alloy. The reason for this study was the limited thickness of the samples in the HPT process. They showed that by this technique, the samples with extraordinarily high thickness to diameter ratio can be examined. Ivansienko et al. [7] introduced high-pressure torsion extrusion (HPTE) for fabricating UFG copper specimens. By performing experiments, they showed that the average grain size of annealed copper was decreased from 26 µm to 350 nm. Zhilyaev et al. [8] studied the electrical conductivity of copper during SPD. They stated that, compared to the initial coarse grains copper, the electrical conductivity of fine-grains copper was not decreased significantly. Straska et al. [9] studied the thermal stability of the UFG microstructure of magnesium AZ31 alloy processed with EX-ECAP. AZ31 alloy was first extruded at 350 °C with an extrusion ratio of 22. Subsequently, it was processed by equal channel angular pressing. In fact, these two processes were performed separately in two different dies. Afsari and Ranaie [10] performed the ECAP process on pure copper up to eight passes at ambient temperature. They stated that after four passes, the grain size was UFG. In addition, after five passes, high hardness and yield strength were obtained, while the electrical conductivity was decreased only about 8% IACS[1]. Damavandi et al. [11] performed the ECAP process on A390 aluminum alloy up to four passes at 400°C. They stated that maximum UTS and elongation values were obtained after third and fourth passes, respectively. They also attributed improvement in the tensile strength and elongation to the grain refinement. Creating UFG copper via SPD has been a well-known topic for researchers during the last decade. Some suggested the repeat of the process for further refinement, while others tried to increase the strength by presenting
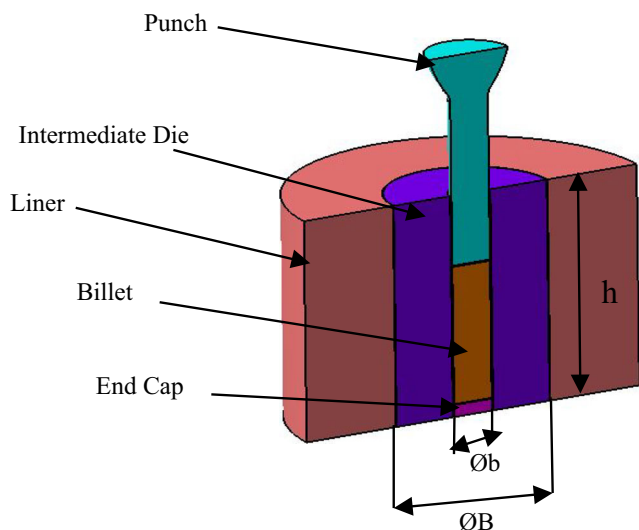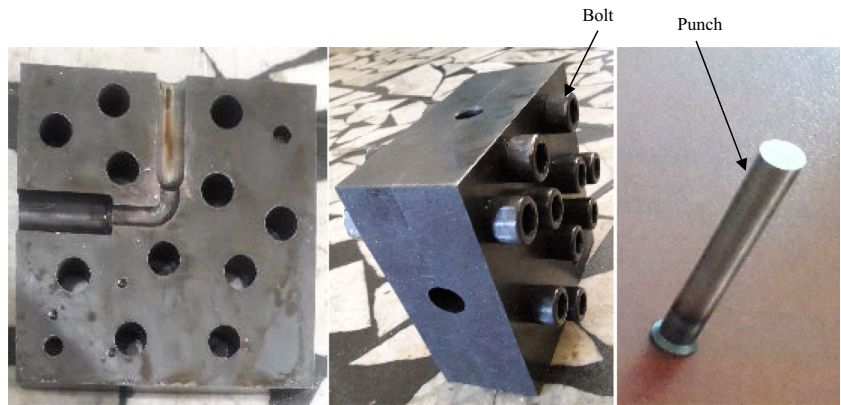

Fig. 2 Schematic of an intermediate die set

---

[1] The International Annealed Copper Standard (IACS)

Table 1 Chemical composition of pure copper

Element	Wt%	Element	Wt%
Zn	0.0051	Al	0.0019
Ni	0.004	Si	0.0014
Pb	0.0027	S	0.0011
P	0.0024	Cu	Rem
Co	0.0019		

Fig. 3 The implemented C-Ex-ECAP die set

different geometries for die shape [12, 13]. The important issue in these processes was to obtain maximum strain and its proper distribution, and increase the strength by applying minimum force, time, cost, and repeating the passes.

The authors [14] proposed the preliminary extrusion-equal channel angular pressing (Ex-ECAP) set-up for fabricating UFG material which is the combination of the two processes of extrusion and ECAP. In fact, these two processes were performed continuously in a single die. The feasibility of this process was performed with AA1050 aluminum alloy. It was concluded that the this process could be used to produce high strength and hardness products but it was not possible to examine the microstructure of the alloy, and thus, it was impossible to examine whether or not the UFG structure could be obtained for the AA1050 alloy. In this study, the abovementioned process is developed more to evaluate the capability and the advantages of the process. In addition, the

microstructural, mechanical, and electrical properties of the pure copper deformed samples have been examined and compared with similar samples formed in the process of ECAP.

2 The principle of C-Ex-ECAP

The schematic of the new C-Ex-ECAP process is shown in Fig. 1, where D is the diameter of the chamber zone (or the initial diameter of the sample), α is the extrusion zone semi-angle, φ is the angle of the die bend, d is the final diameter of the sample, r is the angle of the corner, and L is the land length of the extrusion zone.

As shown in Fig. 1, the new process is a combination of the two processes of extrusion and ECAP. By applying the punch load, the sample passes through the extruded zone and then immediately enters the ECAP zone. The deformed workpiece

Fig. 4 The intermediate die set. **a** Assembled die. **b** Components of the die set
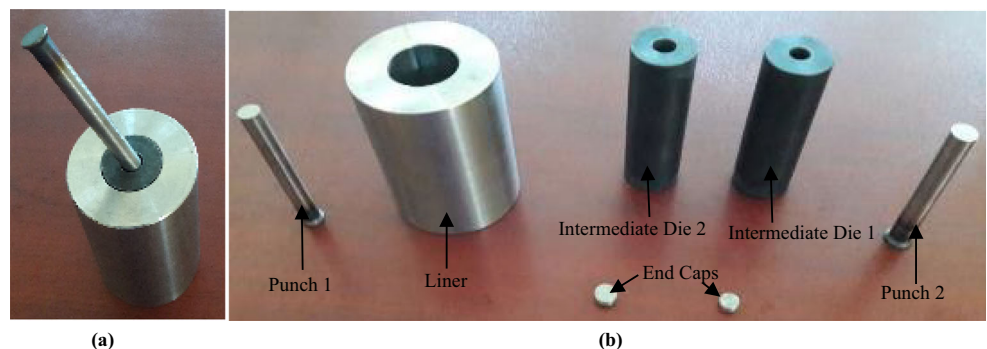
Table 2 Parameters of C-Ex-ECAP die

d (mm)	D (mm)	φ (deg)	α (deg)	r (mm)	L (mm)
10	15	90	120	5	3

Table 3 Characteristics of intermediate dies

Dies	b (mm)	B (mm)	h (mm)
Intermediate 1	12	30	100
Intermediate 2	15	30	100

thus obtained is defined as a half-pass sample. To complete the first pass and perform the next pass, it is required to change the diameter of the sample to its initial diameter. Thus, one or more intermediate dies are needed. The schematic and the corresponding parameters of an intermediate die are shown in Fig. 2. The number of the intermediate dies depends on the length of the output sample from the C-Ex-ECAP die. By increasing the length of the output sample and to prevent buckling, one or more intermediate dies may be needed.

3 Experimental procedure

Pure copper samples with the chemical composition shown in Table 1 were machined to the diameter and length of 15mm and 40mm, respectively. The samples were annealed at 800°C for about 1 h to get the homogenous

microstructure. Figure 3 shows the manufactured C-Ex-ECAP die set, which consists of two halves which are fixed by pins and nuts. By considering the length of the billets, two intermediate dies, shown in Fig. 4, have also been manufactured. The two punches have the diameters of 11.9 and 14.9 mm. All the components of the three dies were manufactured from worked tool steel and hardened to 50 HRc. The parameters of the C-Ex-ECAP die and the intermediate dies are illustrated in Tables 2 and 3, respectively. To minimize the friction between the contact surfaces of the dies and specimens, hydraulic oil was used.

A 600 kN DMG universal testing machine was used to perform the experiments. The C-Ex-ECAP process was carried out up to 6 passes with the ram speed of 10 mm/s. To achieve the initial diameter of the samples with the intermediate dies, a 400 kN hydraulic press was also used.

In order to obtain the mechanical properties of the workpieces, the tensile test was performed using a SANTAM testing machine with a strain rate of 10^{-3} s^{-1} according to ASTM E8 standard [15]. Figure 5 illustrates the tensile test specimen with its dimensions. Table 4 shows the mechanical and thermal properties of the copper sample, and Fig. 6 illustrates its true stress-strain curve.

Vickers micro-hardness (HV) measurement was performed according to ASTM E92 [17] on the cross-section of the samples before and after the C-Ex-ECAP process up to six passes with the force and dwell time of 1 kg and 10 s, respectively.

Samples for microscopic examination were cut perpendicular to the extrusion direction of the billet. After grinding and mechanical polishing, samples were etched within 10–20 s using a solution of 5 gr $FeCl_3$, 15 ml HCl, and 85 ml water.

Fig. 5 **a** The geometry and dimension of tensile test specimen [15]. **b** Photograph of the specimen

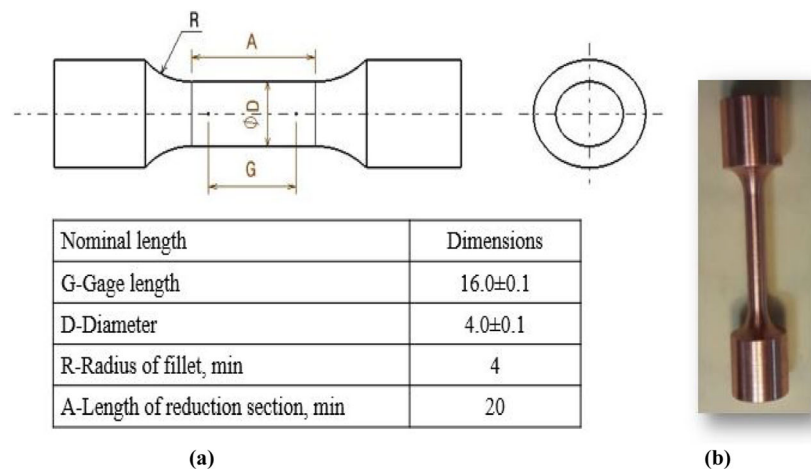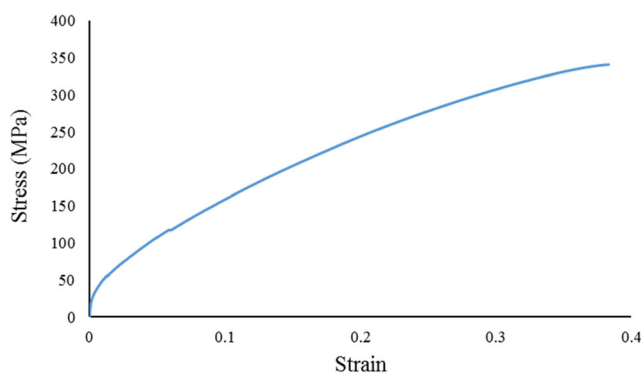| Nominal length	Dimensions
G-Gage length	16.0±0.1
D-Diameter	4.0±0.1
R-Radius of fillet, min	4
A-Length of reduction section, min	20

(a) **(b)**

Table 4 Mechanical and thermal properties of the copper sample

Flow stress (MPa)	$\sigma = 525\varepsilon^{0.35}$	Thermal expansion (mm/(mm °C)) [16]	$\alpha = 1.76\text{e-}5$
Density (kg/m³)	$\rho = 8960$	Thermal conductivity (N/(s °C)) [16]	$\lambda = 43$
Young's modulus (GPa)	$E = 115$	Heat capacity (N/mm² °C) [16]	$C = 3.42$
Poisson s ratio [16]	$\upsilon = 0.33$	Emissivity [16]	$\varepsilon = 0.7$
Initial yield stress (MPa)	$\sigma_y = 35$		

The microstructural observation was carried out using optical microscopy (OM) and scanning electron microscopy (SEM) FEI ESEM QUANTA 200. The average grain size was measured with JMicro Vision software. The tensile fracture surface of the samples was observed by scanning electron microscopy (SEM). Conventional eddy current test was implemented for measuring the changes in electrical properties during the process according to ASTM E1004 [18].

4 Simulation

Microstructure evolution during the forming process directly depends on the effective strain distribution, and to study the deformation behavior, numerical analysis of the effective strain is very important [16, 19]. The numerical study of the C-Ex-ECAP process was carried out using the commercial FE code Deform-3D V11. To model the process, half of the longitudinal cross-section was considered. The pure copper samples were considered to be deformable and were meshed with a total of 32000 tetrahedral elements according to the element sensitivity diagram shown in Fig. 7. The optimal size of the elements was considered to be 0.5 mm. The dies and punches were assumed to be rigid parts. The plasticity behavior of the material has been assumed to

be isotropic. Automatic re-meshing was used to accommodate large strains, and a direct iteration method solver was implemented. The FEM model for one pass of the C-Ex-ECAP process is shown in Fig. 8.

5 Results and discussions

5.1 Verification of simulation

In order to verify the simulation results and obtain an appropriate friction coefficient, the force-displacement curves of the first C-Ex-ECAPed part were obtained from the simulation at different Coulomb friction coefficients and compared with the experimental curves, as illustrated in Fig. 9. It is seen that the curve obtained for the friction coefficient of 0.1 is close to that of the experiment with a maximum deviation of 7%. Thus, the friction coefficient of 0.1 was considered between the die and workpiece in the simulations.

In the FEM simulation, the hardness distribution is consistent with the strain distribution [16]. For more verification of the simulation results, the microhardness test was performed on the sample produced from the first pass. Figure 10 shows the distribution of the effective plastic strain obtained from the simulation and the
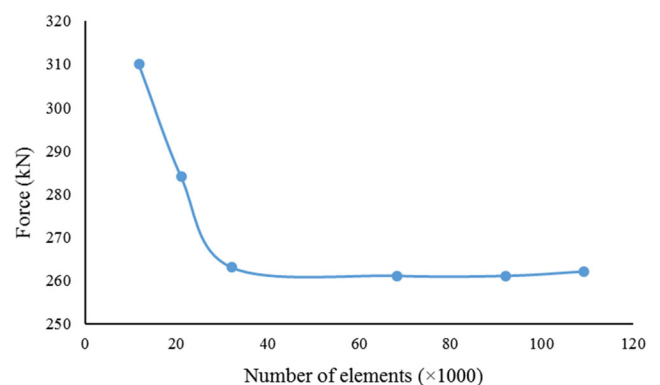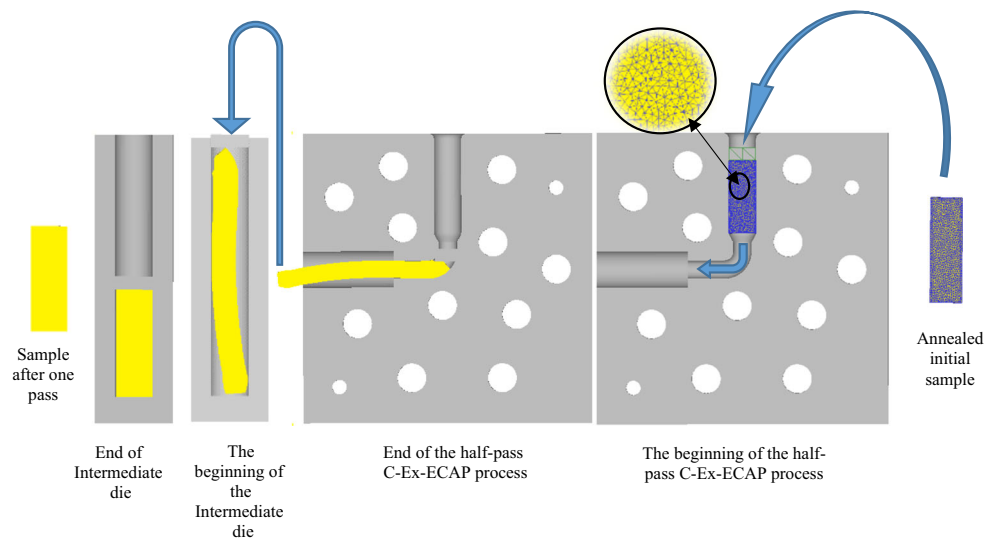

Fig. 6 True stress-strain curve of the annealed sample

Fig. 7 Element sensitivity diagram

Fig. 8 FEM model for one pass of C-Ex-ECAP process

experimentally measured hardness. The hardness and effective strain have similar trends but there is no specific relation between the two curves. In addition, the center of the sample experienced less strain during the process, leading to a smaller hardness compared with the peripheral edge.

5.2 FEM simulation results

Figure 11 illustrates the pure copper deformed sample after one pass of C-Ex-ECAP and the histogram of the strain distribution. It is clear that the effective plastic strain is almost homogenous in the whole regions of the sample which can result in a homogenous hardness along the sample diameter. The amount of average plastic strain in a half-pass and one pass of the C-Ex-ECAP
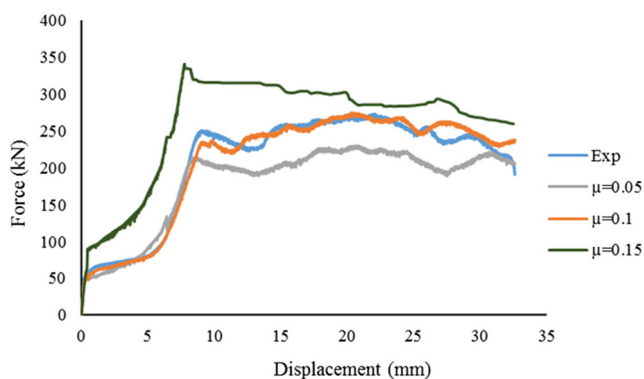

Fig. 9 Force-displacement diagram of the sample after the first pass at different friction coefficients

process is 1.95 and 2.92, respectively. Therefore, the intermediate dies apply the effective plastic strain of 0.97 on the sample. The change of the effective plastic strain in the later half passes and the later one passes of the C-Ex-ECAP process is also 1.95 and 2.92, respectively. This result is in agreement with that reported in [20, 21]. Thus, by performing 6 passes of this process, the average magnitude of effective plastic strain is approximately 17.5. Also, by considering the magnitude of effective plastic strain created in a half-pass, it can be concluded that the C-Ex-ECAP process is a potential method for converting coarse grains to fine grains.

5.3 Comparison between ECAP and C-Ex-ECAP

The same simulation conditions were applied to compare and demonstrate the efficiency of the C-Ex-ECAP process relative to the ECAP process. ECAP die with the same specifications as the ECAP zone of C-Ex-ECAP die (φ=90 deg, r=5, d=10 mm) has been used. The initial sample was considered with a length of 40 mm and a diameter of 10 mm. In the C-Ex-ECAP process, the initial sample was considered with a length of 40 mm and a diameter of D=15 mm and was undergone through the extrusion ratio of 2.25. The final length of the sample is 90 mm which is significantly higher than the ECAPed sample. The results of the simulations of ECAP and C-Ex-ECAP are shown in Fig. 12. Figure 12-a shows a sample after one pass ECAP with the average effective plastic strain of 0.65, while this value for the half-pass of the C-Ex-ECAP according to Fig. 11-a is about 1.95.

Fig. 10 Distribution of effective strain and hardness of the first pass sample in C-Ex-ECAP process
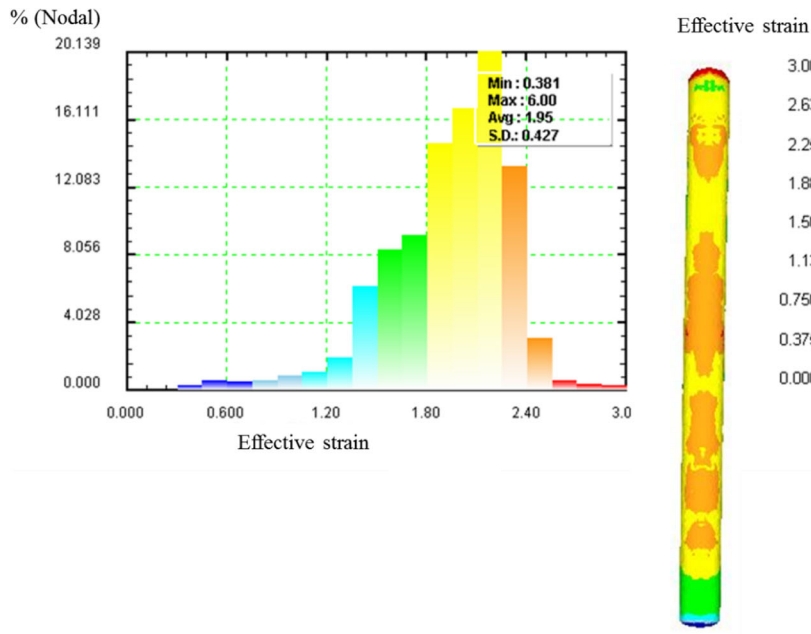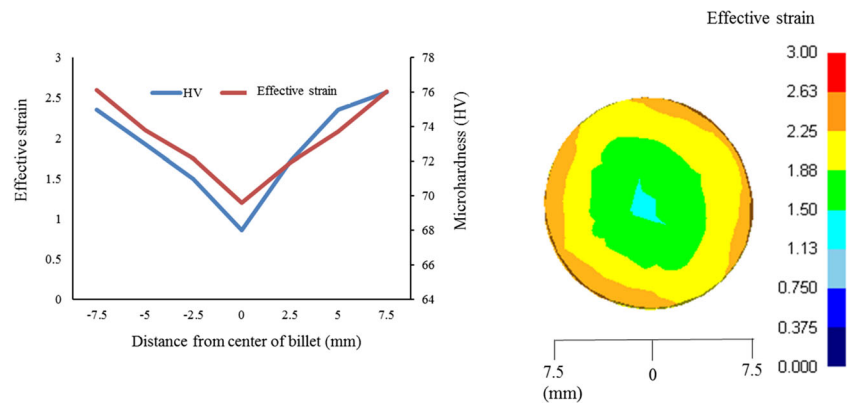
(a)
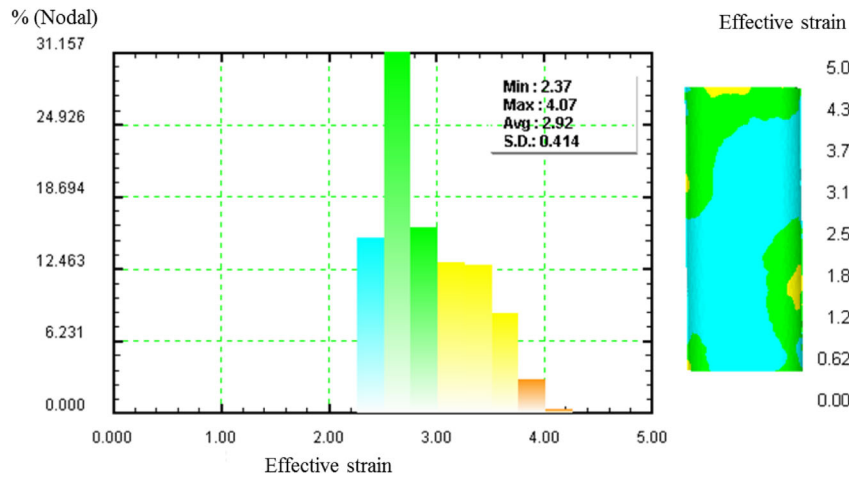
(b)

Fig. 11 Effective strain in C-Ex-ECAP process. **a** half-pass. **b** One pass

Fig. 12 Effective strain distribution. **a** ECAP process. **b** C-Ex-ECAP process
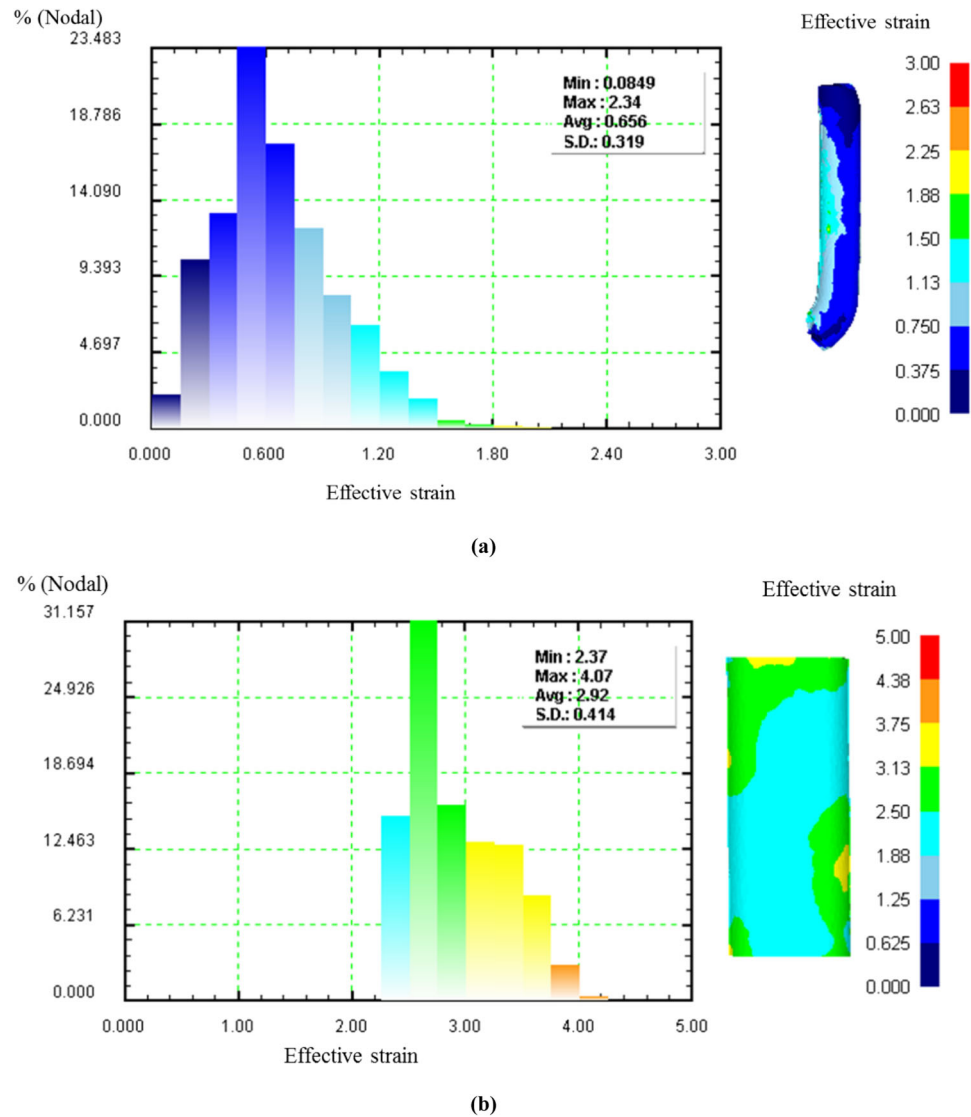

(a)

(b)

Figure 12b shows a sample after one pass C-Ex-ECAP with an average effective plastic strain of 2.92. Also, due to the high friction between the die wall and long samples, the ECAP process has a length limit. This may limit the scale-up in ECAP process, especially as the sample length increases. Thus, the ECAP process is not a suitable method for the production of long UFG materials. Other related techniques such as ECAP-Conform, and ECAP with subsequent rolling, can be used for processing long length UFG materials [22]. In the proposed process, due to the existence of the extrusion zone, by using samples with smaller length, samples with longer length can be achieved, and compared to the ECAP process, there is less limit on the length of the sample. Therefore, there are two advantages in new process compared with ECAP. First, in the C-Ex-ECAP method, the average effective plastic strain is 350% more than that in the ECAP as the result of two severe shear zones in one pass which shows the capability of this process in fabricating UFG and nano-structure materials. Second, due to the existence of the extrusion process at the input of the C-Ex-ECAP, this process is able to produce samples with a longer length than the ECAP.

Figure 13a shows the effective strain applied by different regions of the new process (extrusion zone and extrusion+ ECAP zones=half-pass) on the sample. The average effective plastic strains generated by the extrusion zone alone and extrusion+ ECAP zone are 1.15 and 1.6, respectively.
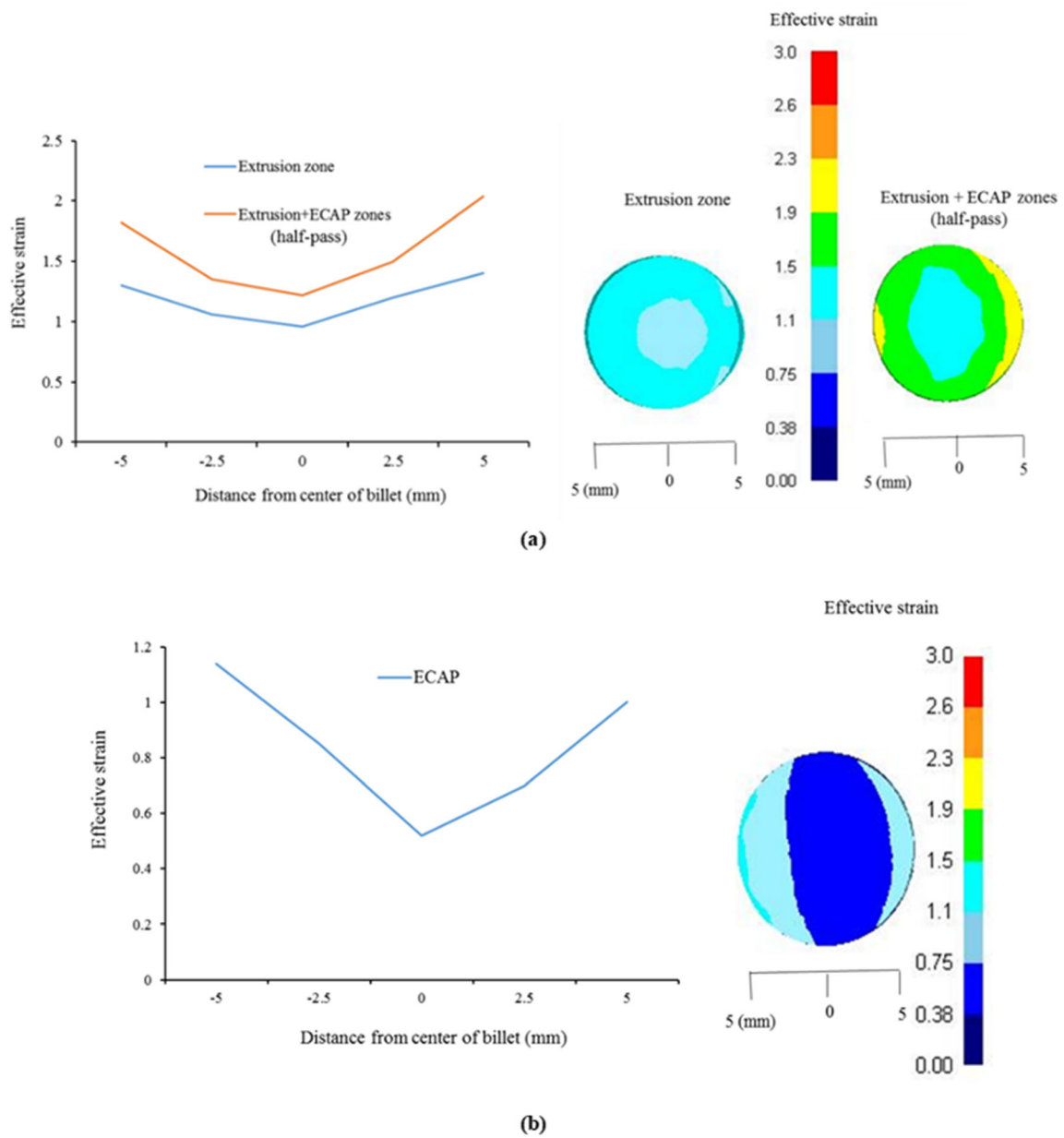
(a)

(b)

Fig. 13 Effective strain distribution. **a** Extrusion zone and extrusion+ECAP zones (half-pass). **b** ECAP process

Fig. 14 a Initial copper sample with the length 40 mm. **b** Sample after first-half pass. **c** Sample after one pass. **d** Sample after second-half pass. **e** Sample after two passes. **f** Sample after four passes. **e** Sample after six passes
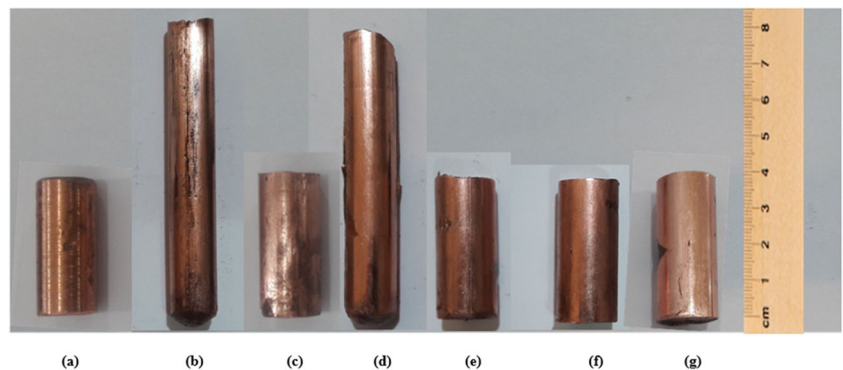
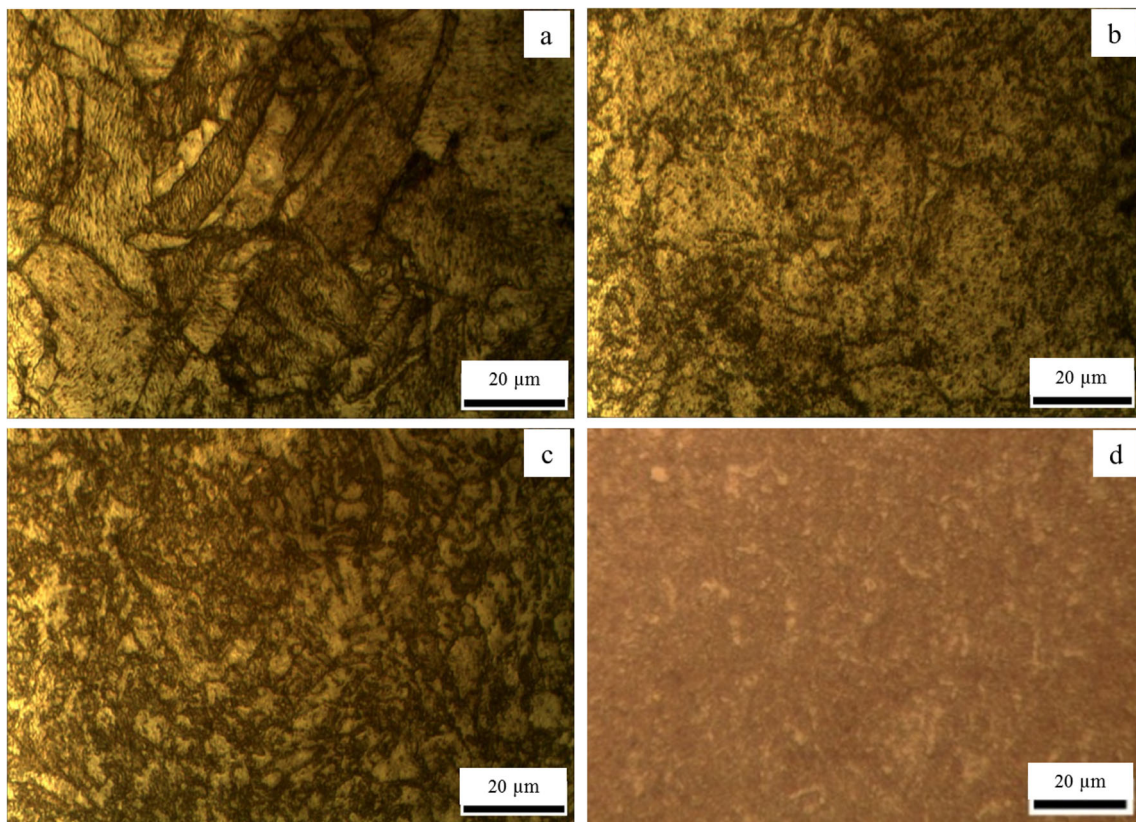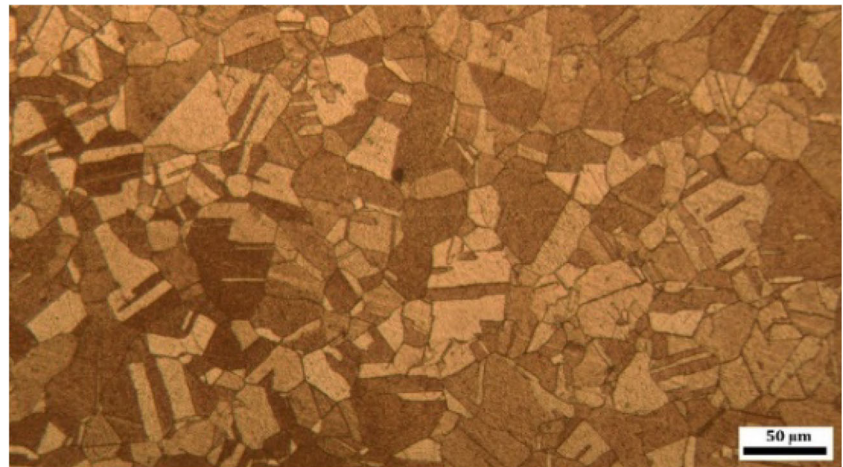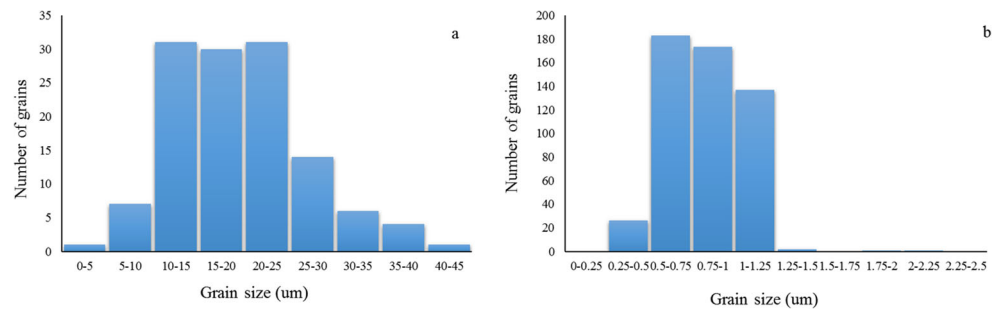**Fig. 15** Optical micrographs of the as-annealed pure copper

Fig. 16 Microstructural images of cross-sections of samples after. **a** One pass. **b** Two passes. **c** Four passes. **d** Six passes

Fig. 17 Grain size distribution in samples. **a** Annealed. **b** After six passes
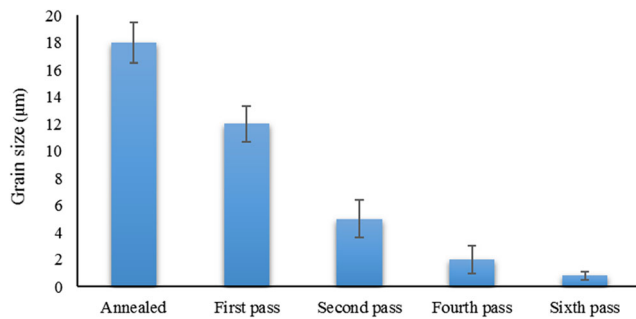
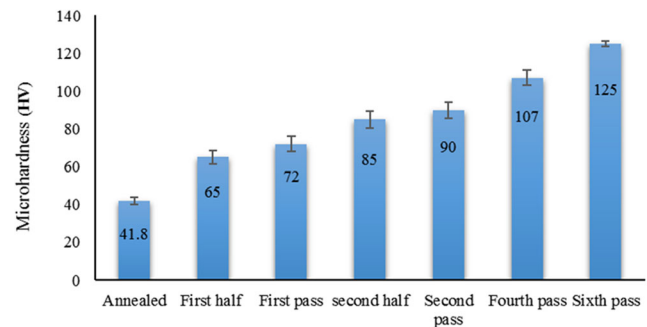**Fig. 18** Mean grain size in the annealed and C-Ex-ECAPed samples

Fig. 20 The average hardness of the sample cross-section in different passes

Figure 13b shows the effective plastic strain distribution of the cross section of the ECAPed sample in Fig. 12a, which is equal to 0.78. According to Fig. 13, compared to the ECAP process, the half-pass of the C-Ex-ECAP process has a uniform effective strain distribution.

Due to the above results, the ECAP zone has less effect on grain refinement due to its larger radius, while the extrusion zone has a greater effect. In addition, as the first pass sample in Fig. 10, the center of the sample experienced less strain during the process, leading to a smaller strain compared with the peripheral edge.

5.4 Microstructure

Figure 14 shows the initial and C-Ex-ECAPed samples. The optical microstructure of the initial sample is illustrated in Fig. 15. The initial microstructure contains coarse and homogenous grains with a few annealing twins. The mean grain size is about 18 μm after the annealing treatment. The microstructure is severely changed after the C-Ex-ECAP process and the process affects the size and shape of grains. The microstructure

of first, second, fourth, and sixth C-Ex-ECAP processed samples is shown in Fig. 16. It is clear that severe grain refinement takes place after the first pass of C-Ex-ECAP and continues slightly up to pass six. As the plastic strain increases during the six passes of the C-Ex-ECAP process, the dislocation density increases, which ultimately leads to the formation of a UFG structure. It is well-accepted that the main mechanism of deformation in copper is dislocation sliding due to its medium stacking fault energy (SFE=78mj m^{-2}) [23]. In general, during the plastic deformation, dislocation cells with high density are produced that collide with each other by applying a higher shear strain (removal or rearrange) and lead to the formation of new high or low angle grain boundaries [24]. Mean grain size reaches to 12 μm after the first pass and also coarse grain is observable after four passes. As shown in Fig. 16c, by increasing the amount of shear strain, the grains are severely deformed. However, complete homogenous grain refinement with equiaxed grains occurred after six passes. This behavior was reported for pure aluminum during the ECAP process which happened at high effective strain (12) where the elongated

Fig. 19 SEM of the cross-section of the sample after six passes with the magnification of **a** ×5000 and **b** ×20,000
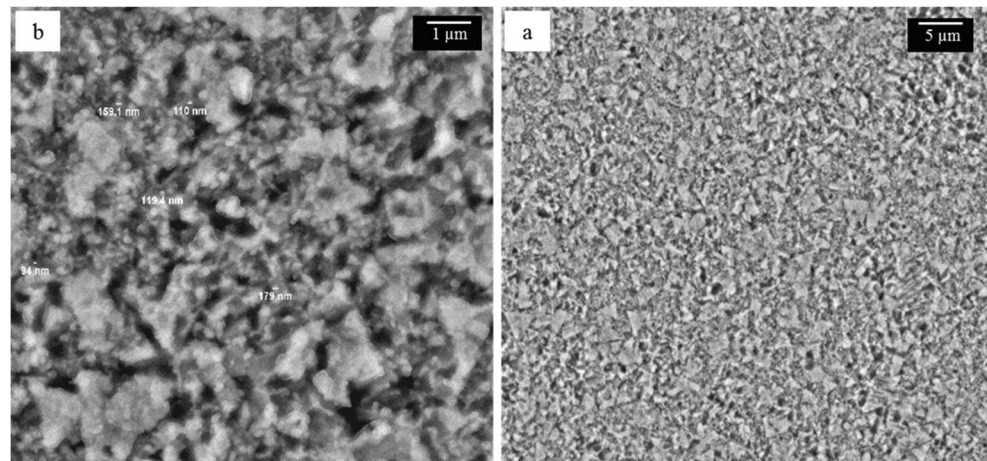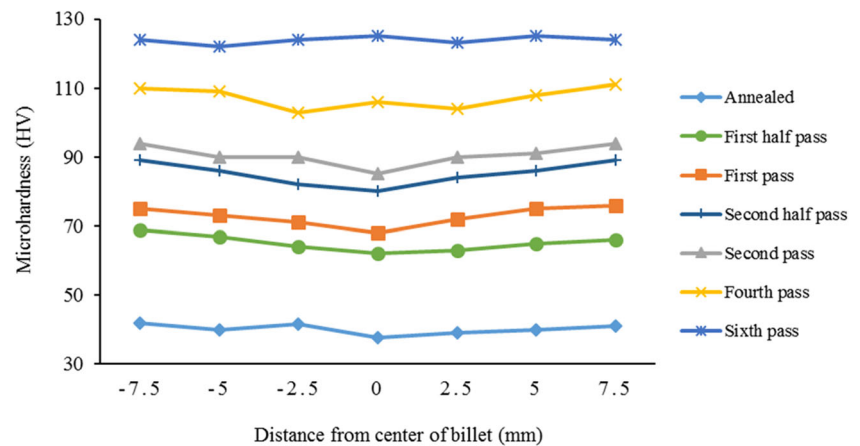
Fig. 21 Hardness distribution on the sample cross-section at different passes

5.5 Mechanical properties

5.5.1 Microhardness

grains were converted to equiaxed grains [25]. Dynamic recrystallization (DRX) is responsible for the formation of fine grains during the severe plastic deformation [26–30].

Grain size distributions of annealed and six passes processed samples are shown in Fig. 17. It is obvious that most grain size in the annealed sample is between 10 and 25 μm and the mean grain size is about 18 μm. After six passes of C-Ex-ECAP, the grain size distributed is between 500 and 1250 nm with a mean grain size of 820 nm. Figure 18 represents the mean grain size distribution for all samples. With increasing the number of passes and effective strain, grain size decreases, and a UFG structure is achieved after six passes. SEM image of a nanostructured sample is shown in Fig. 19 in two magnifications. As it is shown, a large number of grains have nanometer dimensions. This kind of microstructure can affect the mechanical properties of the material, which will be discussed below.
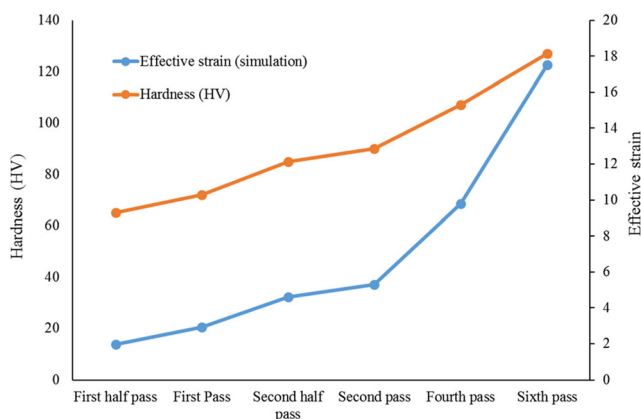
The microhardness (HV) test of the annealed and C-Ex-ECAPed samples was carried out to investigate the process capability of improving the mechanical properties. The average values of microhardness and its distribution on the sample cross-section are presented in Figs. 20 and 21, respectively. It is clear that after the first pass, the hardness increases from the initial value of 41.8 to 65 HV. Also, the hardness increases significantly to 125 HV after 6 passes. In addition, as shown in Fig. 21, the entire cross-section of the samples has almost the same hardness, indicating an almost identical strain distribution. Figure 22 shows the trend of microhardness changes versus simulated effective plastic strain. It also expresses that by increasing the number of passes, the effective strain shows an ascending behavior which is in good agreement with experimental results.
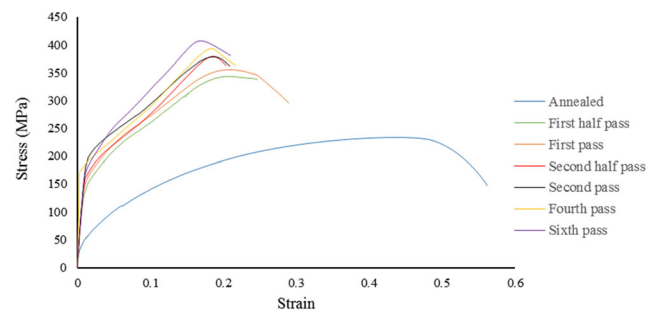

Fig. 22 Effective strain average (simulation) and hardness in C-Ex-ECAP

Fig. 23 Engineering stress-strain curves of the annealed and first-half, one, second-half, two, four, and six passes samples

Table 5 Mechanical properties of the C-Ex-ECAPed pure copper samples

|	Annealed	First-half pass	First pass	Second-half pass	Second pass	Fourth pass	Sixth pass
UTS (MPa)	233.76	343.69	355.69	378.96	379.87	393.5	407.2
YS (MPa)	35	130	135	158	161	167	179
EL%	58.1	27	24	23.2	22.8	9.8	6.5

5.5.2 Tensile test

The influence of the number of C-Ex-ECAP passes on the engineering stress-strain curves is shown in Fig. 23. The yield stress and ultimate tensile strength of the samples increase significantly after this process. Changes in the strength of copper produced up to six passes have been a very increasing trend, but the rate of increase in strength in the first pass is very significant (compared to the annealed sample). The UTS, YS, and elongation of the samples are stated in Table 5. After six passes, the YS and UTS enhance from the initial state of 35 MPa and 233 MPa of the annealed sample to 179 MPa and 407 MPa, respectively, which shows the increase of about 411% and 74%, respectively. However, the elongation decreases from 58.1 to 6.5% during six passes of the C-Ex-ECAP process. This may be related to the presence of shear bands in which they can increase the intensity of planar slip on a grain boundary leading to a low-energy intergranular fracture surface [20]. There are two main reasons for raising the strength after the C-Ex-ECAP process. First, the dislocation density severely increases which results in increasing the strength [31]. Second, according to the Hall-Patch equation, the strength of the material is inversely related to the square of the grain size. In other words, as the grain size decreases, the strength of the material increases [32]. By achieving UFG after six passes of the C-Ex-ECAP process, the role of dislocation in increasing strength and hardness is reduced [33]. This reduces the role of dislocation density in the strength of the material. In other words, with the formation of the UFG structure in the sixth passes, grain boundaries play a main role in the strengthening of materials due to the gradual reduction of grain size. To have a better comparison, Fig. 24 shows the mechanical properties of the samples in one graph. It is seen that, as the number of passes increases, YS and UTS increase, but the elongation decreases. Since materials with ductility of about 10% are suitable for structural materials [34], the pass 4 sample with the ductility of about 10% is a suitable sample of our research for use in structural components.

5.6 Morphology of fracture surfaces

The tensile fracture surfaces were investigated by SEM observations for explaining the fracture mechanism. Figure 25a–e shows the morphology of the fracture surfaces of the annealed and processed samples. Figure 25a is related to the annealed sample with a ductile fracture manner containing deep and

Fig. 24 The mechanical properties of the C-Ex-ECAPed pure copper samples
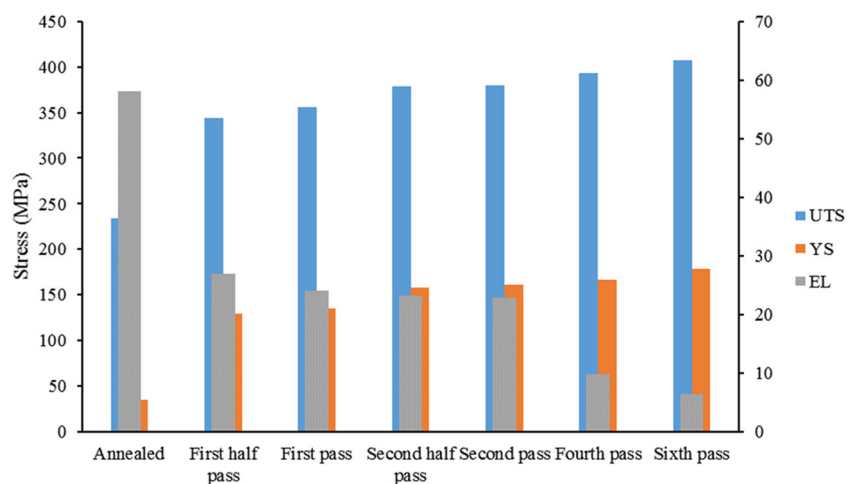
equiaxed dimple with a mean diameter size of 1 to 6 μm. The average dimple size reduces after the first pass of the C-Ex-ECAP process. In other words, the fracture mechanism is affected by the number of C-Ex-ECAP passes. By increasing the number of passes, dimple size remarkably decreases due to high strain and severe grain refinement during the C-Ex-ECAP process, and the samples are less deformed before failure [35]. However, it should be noted that all fracture surfaces show a ductile fracture manner but with various amounts of

deformation. This result was already reported in the previous studies [36–38].

5.7 Electrical conductivity

In general, electrical conductivity reduces after severe plastic deformation as the result of increasing the structural defects and the barriers for electron movement [39]. The electrical conductivity of the different samples is illustrated in Table 6.
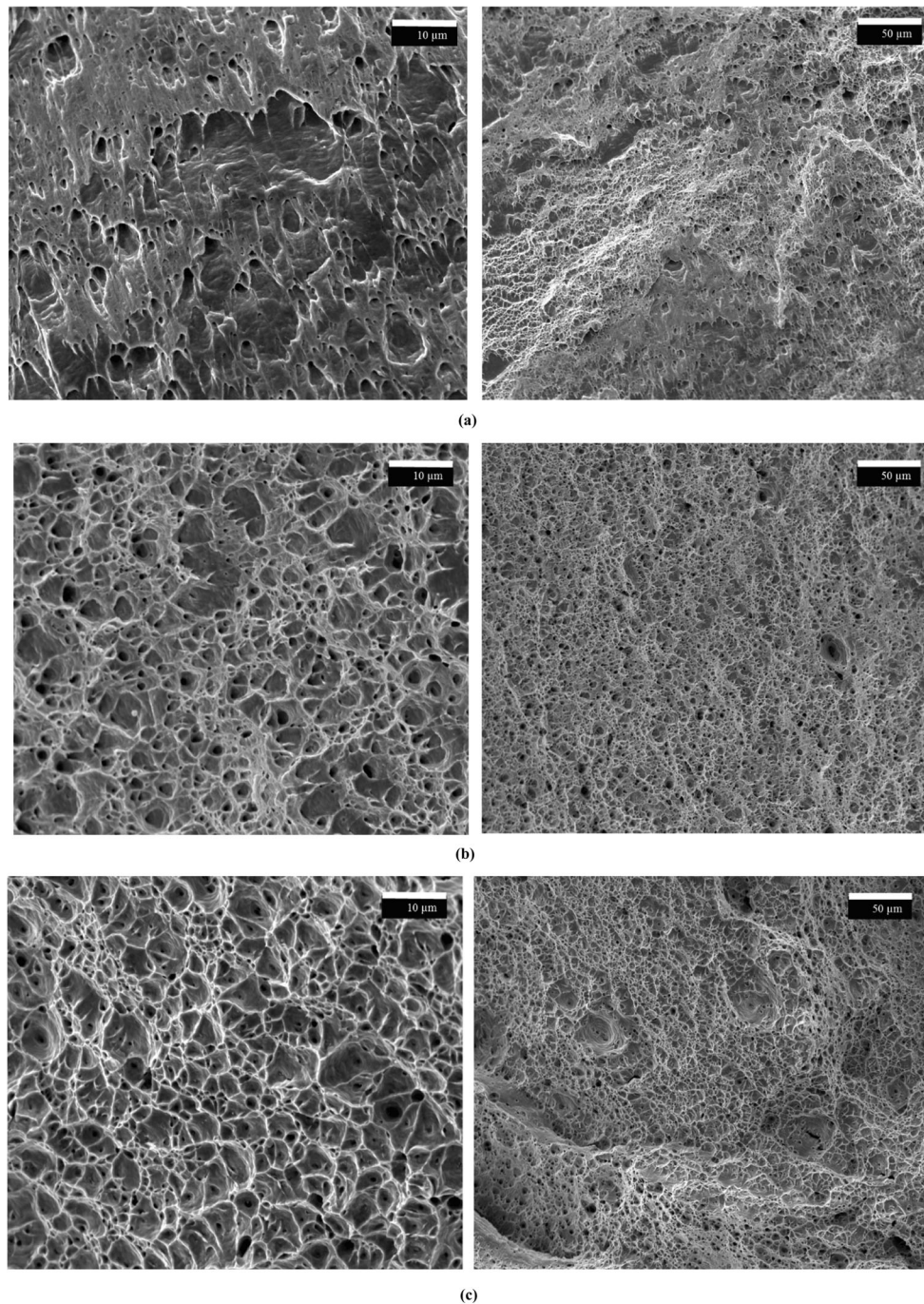

Fig. 25 Tensile fractographs of commercially pure copper. **a** Annealed. **b** First pass. **c** Second pass. **d** Fourth pass. **e** Sixth pass
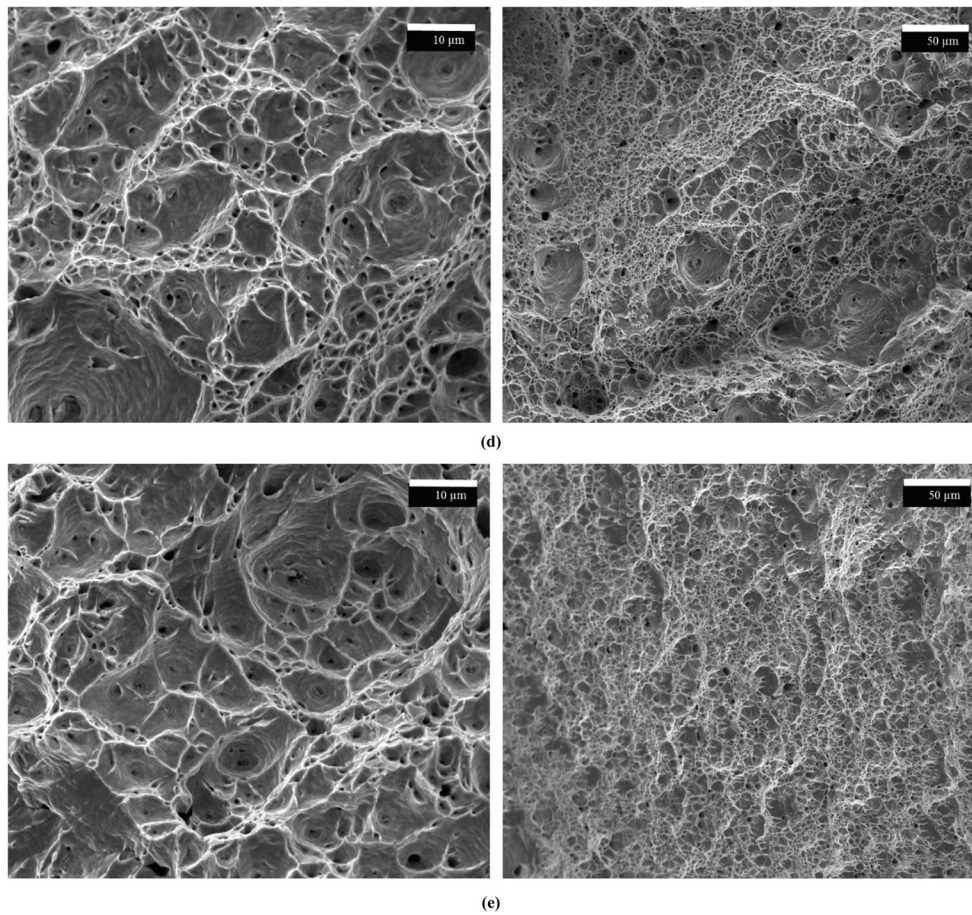
(d)

(e)

Fig. 25 (continued)

It is interesting to note that the electrical conductivity after 6 passes of C-Ex-ECAP is about 90% IACS which is 5.5% less than that of the annealed sample. This indicates that the electrical conductivity has not been changed remarkably despite drastic grain refinement. This marginal difference is attributed to the increasing density of grain boundaries, vacancy, and dislocations. This result demonstrates that C-Ex-ECAP is thoroughly capable of usage in industrial applications.

Table 6 Electrical conductivity of the copper samples

Sample	$(\Omega \, m)^{-1} \times 10^7$	% IACS
Annealed	5.53	95.49
First-half pass	5.44	93.86
First pass	5.42	93.46
Second-half pass	5.39	92.93
Second pass	5.36	92.54
Fourth pass	5.29	91.26
Sixth pass	5.22	90.13

6 Conclusions

The purpose of this article is to present a new forming method by combining the extrusion process and ECAP. In this method, a higher strain is imposed on the material which leads to better homogeneity of microstructure. The results are summarized as follows.

- The proposed C-Ex-ECAP method is capable of fabricating long workpieces with homogenous structure, compared with ECAP.
- The microstructure completely changed during C-Ex-ECAP; after six passes, the samples had UFG structure and the mean grain size reached 820 nm.
- A significant increase took place in the strength and hardness of the sample after the first pass of the process. Based on the results shown in Fig. 20 and Table 5, hardness, ultimate tensile strength, and yield strength enhanced about 200%, 72%, and 411% respectively after 6 passes. Hardness at the peripheral of the sample is greater than that at the center part because the center of the sample experienced less strain during the process.

- Investigation of the fracture surface dimples illustrated a ductile fracture manner in all the samples. Dimples are so deep accompanied with big diameters at the annealed sample. The depth and diameter of these dimples reduced when the sample experienced intense work hardening during the C-Ex-ECAP process.
- Electrical conductivity has not been changed remarkably despite drastic grain refinement.
- The numerical and experimental results provided useful theoretical and experimental guidelines for the C-Ex-ECAP technique, which as a novel SPD method appears very promising for obtaining UFG materials, but changing the diameter with the intermediate die is much too complex for an industrial application, thus extensive basic researches on C-Ex-ECAP are significant to industrial applications in order to overcome this limitation.

7 List of symptoms

σ   Stress (MPa)
ε   Strain

Declarations

References

1. Babaei A, Mashhadi M (2014) Tubular pure copper grain refining by tube cyclic extrusion–compression (TCEC) as a severe plastic deformation technique. Prog Nat Sci Mater Int 24(6):623–630. https://doi.org/10.1016/j.pnsc.2014.10.009

2. Xiong L, Shuai J, Liu K, Hou Z, Zhu L, Li W (2019) Enhanced mechanical and electrical properties of super-aligned carbon nanotubes reinforced copper by severe plastic deformation. Compos Eng 315-320:315–320. https://doi.org/10.1016/j.compositesb.2018.10.023

3. Segal V (1995) Materials processing by simple shear. Mater Sci Eng 197(2):157–164. https://doi.org/10.1016/0921-5093(95)09705-8

4. Wang C, Li F, Li Q, Li J, Wang L, Dong J (2013) A novel severe plastic deformation method for fabricating ultrafine grained pure copper. Mater Des 43:492–498. https://doi.org/10.1016/j.matdes.2012.07.047

5. Ebrahimi M, Djavanroodi F (2014) Experimental and numerical analyses of pure copper during ECFE process as a novel severe plastic deformation method. Prog Nat Sci Mater Int 24(1):68–74. https://doi.org/10.1016/j.pnsc.2014.01.013

6. Hohenwarter A (2015) Incremental high pressure torsion as a novel severe plastic deformation process: processing features and application to copper. Mater Sci Eng 626:80–85. https://doi.org/10.1016/j.msea.2014.12.041

7. Ivanisenko Y, Kulagin R, Fedorov V, Mazilkin A, Scherer T, Baretzky B, Hahn H (2016) High pressure torsion extrusion as a new severe plastic deformation process. Mater Sci Eng 664:247–256. https://doi.org/10.1016/j.msea.2016.04.008

8. Zhilyaev AP, Shakhova I, Belyakov A, Kaibyshev R, Langdon TG (2013) Wear resistance and electro conductivity in copper processed by severe plastic deformation. Wear 305:89–99. https://doi.org/10.1016/j.wear.2013.06.001

9. Straska J, Janecek M, Cizek J, Strasky J, Hadzima B (2014) Microstructure stability of ultra-fine grained magnesium alloy AZ31 processed by extrusion and equal-channel angular pressing (EX–ECAP). Mater Charact 94:69–79. https://doi.org/10.1016/j.matchar.2014.05.013

10. Afsari A, Ranaei MA (2014) Equal channel angular pressing to produce ultrafine pure copper with excellent electrical and mechanical properties. Int Nanosci Nanotechnol 10(4):215–222

11. Damavandi E, Nouroouzi S, Rabiee SM, Jamaati R (2019) Effect of ECAP on microstructure and tensile properties of A390 aluminum alloy. Trans Nonferrous Metals Soc China 29:931–940. https://doi.org/10.1016/S1003-6326(19)65002-8

12. Djavanroodi F, Ebrahimi M (2010) Effect of die parameters and material properties in ECAP with parallel channels. Mater Sci Eng 527(29-30):7593–7599. https://doi.org/10.1016/j.msea.2010.08.022

13. IbrahimAbd EL AAL M (2017) 3D FEM simulation and experimental validation of plastic deformation of pure-alumimum deformed by ECAP and combination of ECAP and direct extrusion. Trans Nonferrous Metals Soc Chin 27:1338–1352. https://doi.org/10.1016/S1003-6326(17)60155-9

14. Akbarzadeh B, Gorji H, Bakhshi-Jooybari M, Jamaati R, Mirnia MJ (2020) Development of a new process for the severe plastic deformation of AA 1050 to improve the mechanical properties. Iran J Manag Eng 7(4):19–29 (in Persian)

15. ASTM E8 / E8M-16ae1 (2016) Standard test methods for tension testing of metallic materials. ASTM International, West Conshohocken. https://doi.org/10.1520/E0008_E0008M-16AE01

16. Wang C, Li F, Li Q, Wang L (2012) Numerical and experimental studies of pure copper processed by a new severe plastic deformation method, Severely deformed copper by equal channel angular pressing. Mater Sci Eng 548:19–26. https://doi.org/10.1016/j.msea.2012.03.055

17. ASTM E92-17 (2017) Standard test methods for vickers hardness and knoop hardness of metallic materials. ASTM International, West Conshohocken. https://doi.org/10.1520/E0092-17

18. ASTM E1004-17 (2017) Standard test method for determining electrical conductivity using the electromagnetic (Eddy Current) method. ASTM International, West Conshohocken. https://doi.org/10.1520/E1004-17

19. Faraji G, Babaei A, Mashhadi MM, Abrinia K (2012) Parallel tubular channel angular pressing (PTCAP) as a new severe plastic deformation method for cylindrical tubes. Mater Lett 77:82–85. https://doi.org/10.1016/j.matlet.2012.03.007

20. Ebrahimi M, Gode C (2017) Severely deformed copper by equal channel angular pressing. Prog Nat Sci Mater Int 27:244–250. https://doi.org/10.1016/j.pnsc.2017.03.002

21. Iwahashi Y, Wang J, Horita Z, Nemoto M, Langdon TG (1996) Principle of equal-channel angular pressing for the processing of ultra-fine grained materials. Scr Mater 35(2):143–146. https://doi.org/10.1016/1359-6462(96)00107-8

22. Riazat M, Faraji G (2015) Size effect in equal channel angular pressing (ECAP) process. J Adv Mater Process 3(3):3–12

23. Habibi A, Ketabchi M, Eskandarzadeh M (2011) Nano-grained pure copper with high-strength and high-conductivity produced by equal channel angular rolling process. Mater Process Technol 211(6):1085–1090. https://doi.org/10.1016/j.jmatprotec.2011.01.009

24. Kommel L, Hussainova I, Volobueva O (2007) Microstructure and properties development of copper during severe plastic deformation. Mater Des 28(7):2121–2128. https://doi.org/10.1016/j.matdes.2006.05.021

25. Wei W, Wei K, Fan G (2008) A new constitutive equation for strain hardening and softening of fcc metals during severe plastic deformation. Acta Mater 56(17):4771–4779. https://doi.org/10.1016/j.actamat.2008.05.025

26. Ferrasse S, Segal VM, Hartwig KT, Goforth R (1997) Microstructure and properties of copper and aluminum alloy 3003 heavily worked by equal channel angular extrusion. Metall Mater Trans A 28(A):1047–1057. https://doi.org/10.1007/s11661-997-0234-z

27. Li BL, Shigeiri N, Tsuji N, Minamino Y (2006) Microstructural evolution in pure copper severely deformed by the ARB process. Mater Sci Forum 503(504):615–620. https://doi.org/10.4028/www.scientific.net/MSF.503-504.615

28. Wang YM, Ma E (2004) Three strategies to achieve uniform tensile deformation in a nanostructured metal. Acta Mater 52:1699–1709. https://doi.org/10.1016/j.actamat.2003.12.022

29. Mishra A, Kad BK, Gregori F, Meyers MA (2007) Microstructural evolution in copper subjected to severe plastic deformation: experiments and analysis. Acta Mater 55:13–28. https://doi.org/10.1016/j.actamat.2006.07.008

30. Xu J, Jianwei L, Shan D, Guo B (2016) Microstructural evolution and micro/meso-deformation behavior in pure copper processed by equal-channel angular pressing. Mater Sci Eng 664:114–125. https://doi.org/10.1016/j.msea.2016.03.016

31. Zhu CF, Du FP, Jiao QY, Wang XM, Chen AY, Liu F, Pan D (2013) Microstructure and strength of pure Cu with large grains processed by equal channel angular pressing. Mater Des 52:23–29. https://doi.org/10.1016/j.matdes.2013.05.029

32. Hansen N (2004) Hall–Petch relation and boundary strengthening. Scr Mater 51:801–806. https://doi.org/10.1016/j.scriptamat.2004.06.002

33. Valiev RZ, Alexandrov IV, Zhu YT, Lowe TC (2002) Paradox of strength and ductility in metals processed by severe plastic deformation. Mater Res 17:5–8. https://doi.org/10.1557/JMR.2002.0002

34. Dao M, Lu L, Asaro RJ, De Hosson JTM, Ma E (2007) Toward a quantitative understanding of mechanical behavior of nanocrystalline metals. Acta Mater 55:4041–4065. https://doi.org/10.1016/j.actamat.2007.01.038

35. Fata A, Faraji G, Mashhadi MM, Tavakoli V (2017) Hot deformation behavior of Mg-Zn Al alloy tube processed by severe plastic deformation. Arch Metall Mater 62:159–166. https://doi.org/10.1515/amm-2017-0022

36. Fang DR, Duan QQ, Zhao NQ, Li JJ, Wu SD, Zhang ZF (2007) Tensile properties and fracture mechanism of Al–Mg alloy subjected to equal channel angular pressing. Mater Sci Eng 459:137–144. https://doi.org/10.1016/j.msea.2007.01.062

37. Ko YG, Shin DH, Park KT, Lee CS (2006) An analysis of the strain hardening behavior of ultra-fine grain pure titanium. Scr Mater 54:1785–1789. https://doi.org/10.1016/j.scriptamat.2006.01.034

38. Vinogradov A, Ishida T, Kitagawa K, Kopylov V (2005) Effect of strain path on structure and mechanical behavior of ultra-fine grain Cu–Cr alloy produ ced by equal-channel angular pressing. Acta Mater 53:2181–2192. https://doi.org/10.1016/j.actamat.2005.01.046

39. Lipinska M, Olejnik L, Lewandowska M (2018) The influence of an ECAP-based deformation process on the microstructure and properties of electrolytic tough pitch copper. Mater Sci 53:3862–3875. https://doi.org/10.1007/s10853-017-1814-y